© 2022. Published by The Company of Biologists Ltd | Journal of Cell Science (2022) 135, jcs259097. doi:10.1242/jcs.259097

RESEARCH ARTICLE

TAZ exhibits phase separation properties and interacts with Smad7 and β-catenin to repress skeletal myogenesis

Soma Tripathi[1,2,3,*], Tetsuaki Miyake[1,2,3,*], Jonathan Kelebeev[1,2,3] and John C. McDermott[1,2,3,4,‡]

ABSTRACT

Hippo signaling in *Drosophila* and mammals is prominent in regulating cell proliferation, death and differentiation. Hippo signaling effectors (YAP and TAZ; also known as YAP1 and WWTR1, respectively) exhibit crosstalk with transforming growth factor-β (TGF-β)–Smad and Wnt/β-catenin pathways. Previously, we implicated Smad7 and β-catenin in mammalian myogenesis. Therefore, we assessed a potential role of TAZ on the Smad7–β-catenin complex in muscle cells. Here, we document functional interactions between Smad7, TAZ and β-catenin in mouse myogenic cells. Ectopic TAZ expression resulted in repression of the muscle-specific creatine kinase muscle (*Ckm*) gene promoter and its corresponding protein level. Depletion of endogenous TAZ enhanced *Ckm* promoter activation. Ectopic TAZ, while potently active on a TEAD reporter (HIP-HOP), repressed myogenin (*Myog*) and *Myod1* enhancer regions and myogenin protein level. Additionally, a Wnt/β-catenin readout (TOP flash) demonstrated TAZ-mediated inhibition of β-catenin activity. In myoblasts, TAZ was predominantly localized in nuclear speckles, while in differentiation conditions TAZ was hyperphosphorylated at Ser89, leading to enhanced cytoplasmic sequestration. Finally, live-cell imaging indicated that TAZ exhibits properties of liquid–liquid phase separation (LLPS). These observations indicate that TAZ, as an effector of Hippo signaling, suppresses the myogenic differentiation machinery.

KEY WORDS: WW domain-containing transcription regulator protein 1, TAZ, Smad7, β-catenin, Myogenesis, Transcription, Liquid–liquid phase separation, LLPS, *Creatine kinase muscle, ckm*

INTRODUCTION

Development and maintenance of tissues and organs requires a delicate balance between proliferation, apoptosis and differentiation (Varelas, 2014). A search for mutations that cause tissue overgrowth in *Drosophila melanogaster* precipitated the discovery of a conserved kinase cascade comprising of Hippo and Warts kinase and adaptor proteins Salvador and Mob (Jia et al., 2003; Justice et al., 1995; Pantalacci et al., 2003; Tapon et al., 2002; Udan et al., 2003; Wu et al., 2003), collectively referred to as Hippo signaling. Activation of Hippo signaling promotes activation of Hippo kinases resulting in phosphorylation of a transcriptional regulator, Yorkie, and its subsequent sequestration in the cytoplasm, thus inhibiting its functional association with another transcription factor (Scalloped) (Huang et al., 2005). Yes-associated protein (YAP; also known as YAP1), is the mammalian homolog of Yorkie in vertebrates, and MST1 and MST2 (STK4 and STK3), and LATS1 and LATS2 are homologs of the *Drosophila* Hippo kinases, indicating the evolutionary conservation of Hippo signaling (Sudol, 1994; Sudol et al., 1995). TAZ (also known as WWTR1), a paralog of YAP in vertebrates, was subsequently characterized as a novel transcriptional co-activator regulated by interactions with 14-3-3 and PDZ domain proteins (Kanai et al., 2000). TAZ phosphorylation on a conserved serine residue (Ser89 in human TAZ; equivalent to Ser127 in human YAP) results in inhibition of TAZ transcriptional co-activation through 14-3-3 protein-mediated cytoplasmic retention.

A number of studies have proposed extensive crosstalk between Hippo signaling and other cellular signaling pathways. Documentation of crosstalk between TGF-β and Hippo signaling was first reported in a yeast two-hybrid screen where YAP1 was identified as a novel Smad7-interacting protein (Ferrigno et al., 2002). In *Drosophila*, Yorkie interacts with and promotes Mad-dependent transcription in response to DPP signaling (Alarcon et al., 2009; Oh and Irvine, 2011). In another high-throughput screen aimed at identifying novel regulators of TGF-β signaling in human embryonic cells, TAZ was identified as a mediator of Smad (the vertebrate homolog of MAD) nucleocytoplasmic shuttling that is essential for TGF-β signaling. YAP was also shown to bind BMP-regulated Smad1, Smad5 and Smad8 and TGF-β regulated Smad2 and Smad3. The YAP–Smad1 complex is regulated by the mediator-associated kinases CDK8 and CDK9, which phosphorylate the Smad1 linker domain to expose a PPXY motif and promote binding to the YAP WW domains (Alarcon et al., 2009). Thus, there is extensive documented crosstalk between the Hippo and TGF-β pathways.

In the absence of Wnt signaling, components of the β-catenin destruction complex have been shown to sequester TAZ, promoting its degradation. β-catenin contributes to this by bridging TAZ to the ubiquitin ligase β-TrCP (Azzolin et al., 2014). Receptor activation by Wnt ligands, allows escape of β-catenin from its destruction complex, which concomitantly also stabilizes TAZ expression, thereby promoting nuclear accumulation of both β-catenin and TAZ (Azzolin et al., 2012). TAZ-mediated transcription and protein stabilization are a general feature of the Wnt response in a variety of cellular model systems suggesting that the β-catenin–TCF complex is not the sole modality by which the Wnt/β-catenin pathway can regulate gene expression. Hence, Wnt signaling can promote the nuclear accumulation of both β-catenin and TAZ. The consequences of crosstalk between these signaling pathways is of particular interest for skeletal muscle biology given that TGF-β, Wnt and Hippo signaling have all been implicated in regulating various

[1]Department of Biology, York University, Toronto, ON, M3J 1P3, Canada. [2]Muscle Health Research Centre (MHRC), York University, Toronto, ON, M3J 1P3, Canada. [3]Centre for Research in Biomolecular Interactions (CRBI), York University, Toronto, ON, M3J 1P3, Canada. [4]Centre for Research in Mass Spectrometry (CRMS), York University, Toronto, ON, M3J 1P3, Canada.
*These authors contributed equally to this work

‡Author for correspondence (jmcderm@yorku.ca)

J.C.M., 0000-0001-9696-8929

Handling Editor: Jennifer Lippincott-Schwartz
Received 6 July 2021; Accepted 18 November 2021

Journal of Cell Science (2022) 135, jcs259097. doi:10.1242/jcs.259097

aspects of skeletal muscle development and post-natal physiology (Rodriguez et al., 2014; Suzuki et al., 2015; Wackerhage et al., 2014; Watt et al., 2018).

Therefore, in view of the putative connections between TAZ and both Smad7 and β-catenin, we questioned whether TAZ modulates the function of Smad7 and β-catenin in myogenic cells that we have previously reported (Tripathi et al., 2019). Here, we document a protein–protein interaction between Smad7 and TAZ in mouse muscle cells which functions to repress Smad7 and β-catenin function at muscle-specific promoters, such as the well-characterized muscle creatine kinase (*Ckm*) gene. In these studies, we also document that TAZ exhibits robust phase separation properties in myogenic cells. Collectively, these observations are consistent with the role of Hippo signaling in myogenic cells which, when off, promotes proliferation due to TAZ nuclear accumulation and activation of genes associated with proliferation, which is consistent with results from a previous study in which both Yap and TAZ were documented to enhance proliferation of satellite cells (Sun et al., 2017). We now propose that, as well as positively enhancing the expression of proliferative genes, nuclear TAZ also suppresses differentiation by acting as a co-repressor of the myogenic transcription complex containing Smad7 and β-catenin. Thus, our data indicate that, when Hippo signaling is activated, TAZ is phosphorylated and retained in the cytoplasm, which concomitantly de-represses the nuclear activity of Smad7 and β-catenin at muscle promoters. These data support a model in which TAZ acts as a fulcrum to balance the ratio of proliferation and differentiation in myogenic cells. These studies identify TAZ as a potential determinant of muscle differentiation, having implications for control of muscle mass during development, growth and regeneration.

RESULTS

Smad7 and TAZ interact in myogenic cells

Previously, the Hippo effector Yap was identified as a novel Smad7-interacting protein in Cos-7 cells (Ferrigno et al., 2002). We initially tested whether the YAP paralog TAZ also interacts with Smad7 since TAZ is expressed at a much higher level than YAP in muscle cells and, by immunofluorescence analysis, the nuclear accumulation of TAZ is reduced in differentiating cells (Fig. 1A,B). We have previously documented that Smad7 is expressed in muscle cells and plays an important role in muscle-specific gene transcription (Kollias et al., 2006; Miyake et al., 2010; Tripathi et al., 2019) and this has been confirmed *in vivo* (Cohen et al., 2015). Here, we show that TAZ is expressed in both proliferation and differentiation stages of cultured C2C12 muscle cells, and the nuclear accumulation of TAZ is reduced in differentiation conditions (Fig. 1A). To initially test for the interaction between TAZ and Smad7 biochemically, Flag–Smad7 was ectopically expressed in C2C12 cells, and total protein lysates were subjected to immunoprecipitation (IP) using anti-Flag magnetic beads. Lysate from ectopically expressed Flag–Trim28 was used as a negative control. Immunoblot analysis of the eluates from the Flag–Smad7 IP, but not from Flag–Trim28 IP revealed the presence of TAZ, indicating that they are potentially constituents of the same protein complex (Fig. 1B). Therefore, we hypothesized that TAZ modulates the myogenic transcriptional complex that we and others have previously documented (Rampalli et al., 2007; Tripathi et al., 2019; see schematic in Fig. 1C).

TAZ antagonizes the myogenic function of Smad7

Previously, we documented the contribution of Smad7 to the transcriptional control of the muscle creatine kinase (*Ckm*) promoter in co-operation with MyoD (also known as MyoD1) and β-catenin (Fig. 1C; Tripathi et al., 2019). The *Ckm* promoter has been used in many studies in the myogenesis field as a paradigm of muscle-specific transcriptional control. We therefore tested whether TAZ could modulate this complex through its interaction with Smad7. Ectopic expression of TAZ alone or in combination with Smad7 demonstrated that TAZ potently inhibits the transcriptional induction of *Ckm* by Smad7 (Fig. 2A). To further validate these observations, we utilized two independent TAZ-directed siRNAs to deplete the levels of endogenous TAZ (Fig. 2B) and then performed the *Ckm* luciferase reporter assay in TAZ-depleted versus normal cells. Depletion of endogenous TAZ enhanced *Ckm* transcriptional activity by Smad7 (Fig. 2C,D). Moreover, depletion of endogenous TAZ resulted in an overall enhancement of *Ckm* transcriptional activity (Fig. 2C,D). In addition, ectopic TAZ expression resulted in a corresponding reduction in CKM protein level in a differentiation time course experiment (Fig. 2E; Fig. S2 documents total protein in this assay confirming the CKM downregulation in TAZ-expressing cells). It should be noted that the transfection efficiency for ectopic TAZ expression is not complete, and we suggest that the residual CKM expression is likely derived from the untransfected cells. Collectively, these data support a repressive role of TAZ during muscle cell differentiation. These data also confirm a previous study in which the repressive role of TAZ on myogenesis was observed (Huraskin et al., 2016).

TAZ inhibits the activity of a Smad7–β-catenin complex

Given that our previous study reported a direct interaction between Smad7 and β-catenin and their functional co-operativity is required for their function on the *Ckm* promoter, we determined whether TAZ can directly target β-catenin activity using a more specific assay system. For this, we utilized the TOP flash reporter gene that contains multimerized binding sites for TCF/LEF, which serve as an indicator of β-catenin-mediated transcriptional activation. FOP flash contains mutated TCF/LEF-binding sites serving as a corresponding negative control in this assay (Anand et al., 2011). Ectopic expression of TAZ resulted in robust inhibition of β-catenin activity (Fig. 3A), while no appreciable effect of TAZ was observed on the FOP flash reporter gene (Fig. S1). Protein level expression of exogenous constructs was confirmed by western blot analysis (Fig. 3A, lower panels). These data indicate that TAZ specifically represses β-catenin-induced transcriptional activation. Next, we tested whether the TAZ S89A mutation inhibits β-catenin activity similar to wild type, which it did (Fig. 3B). The logic of using TAZ S89A was based on its property of evading the cytoplasmic degradation machinery, which has previously been shown to modulate the protein levels of both β-catenin and TAZ. These data indicate that the inhibitory effect of TAZ on β-catenin transcriptional activation does not appreciably involve the cytoplasmic degradation machinery affecting β-catenin levels. This is also supported in the protein blots, which show that ectopic expression of TAZ did not affect endogenous or exogenously transfected β-catenin levels (Fig. 3A). Next, since TAZ is perhaps better known for its role as a transcriptional co-activator, we tested whether TAZ enhances the well-characterized HIP/HOP reporter gene system in the same cellular system. HOP is comprised of multimerized TEAD-binding sites driving a *luc* reporter gene, which serves as a readout for YAP/TAZ activity (HIP is the same reporter gene, but with mutated TEAD sites serving as a negative control) (Kim and Gumbiner, 2015). In this assay, we observed that both wild-type TAZ and TAZ S89A robustly activate the HOP reporter gene under the same cellular conditions in which

Journal of Cell Science (2022) 135, jcs259097. doi:10.1242/jcs.259097

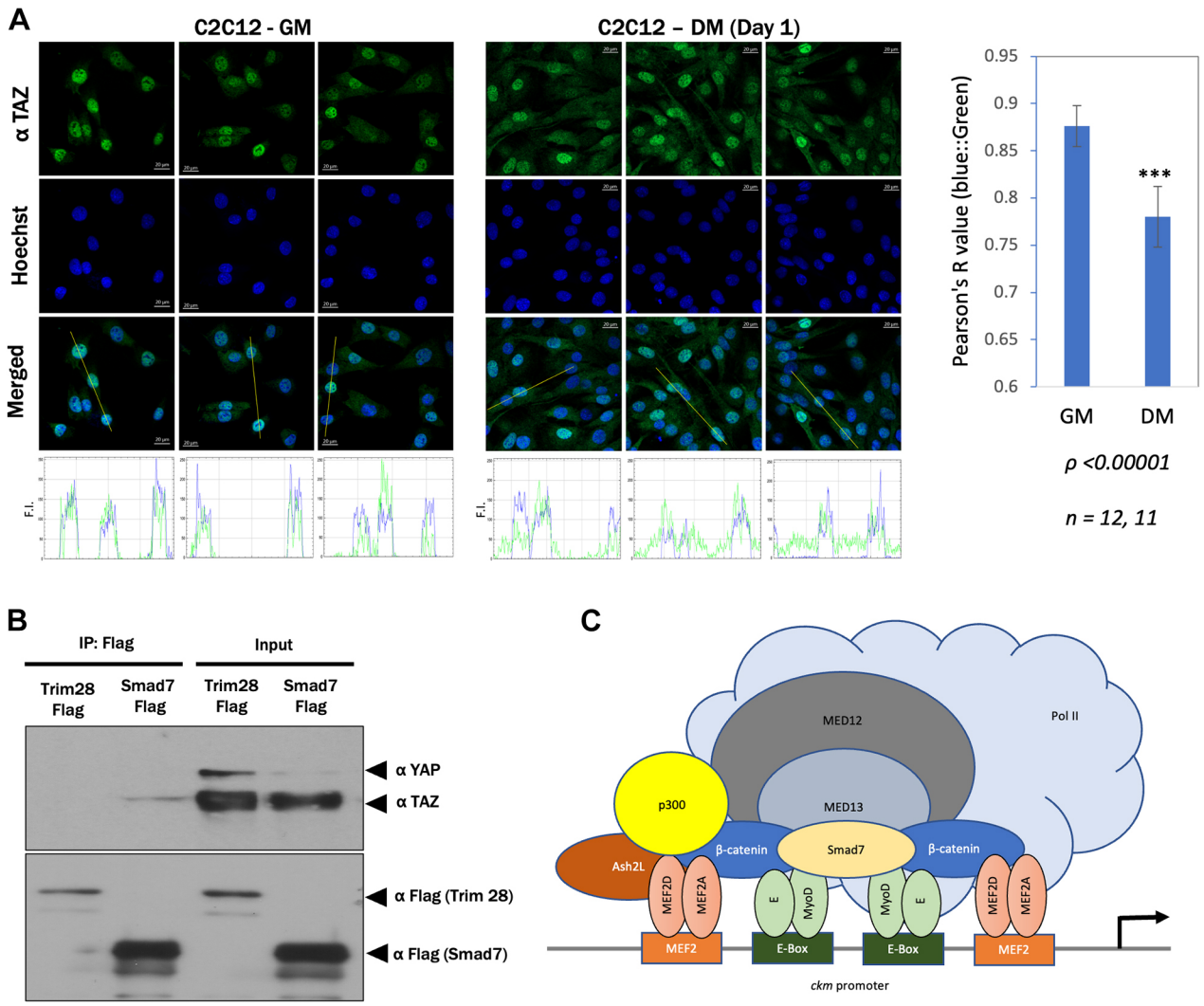

Fig. 1. Biochemical interaction between Smad7 and TAZ. (A) Immunofluorescence analysis of C2C12 myogenic cells during myogenic differentiation. C2C12 myoblasts were grown in growth medium (GM) and changed to differentiation medium (DM) to initiate the differentiation program. Cells were stained for TAZ and Hoechst 33342 to detect nuclei. Nuclear localization of TAZ was assessed by line scan analysis and the Pearson's R value of the overlap between TAfZ (green) and nuclear (Hoechst; blue) signals was carried out using ImageJ. F.I., fluorescence intensity. Statistical analysis (***P<0.00001) of the two groups (GM; n=12) and (DM; n=11) was calculated by one-way ANOVA. (B) C2C12 myoblasts were transiently transfected with Smad7–Flag. Smad7–Flag lysates were utilized for Co-IP with anti-Flag magnetic beads and eluates were probed with TAZ or Flag antibody to detect the possible interaction with Smad7. IP with lysates from Trim28–Flag transfected cells served as a negative control. Blot is representative of n=6 immunoprecipitations for TAZ interaction with Flag–Smad7. In this particular blot Trim28 was used as a negative control (n=1). (C) A schematic view of a myogenic 'holocomplex' on the *Ckm* promoter. Scale bars: 20 µm.

we documented repression of the β-catenin-dependent TOP flash reporter gene (Fig. 3C). Thus, these data indicate that whereas TAZ strongly represses β-catenin activity in muscle cells, it conversely potently activates the Hippo-responsive HIP reporter system under identical cellular conditions. We went on to further test whether TAZ S89A represses some other well-characterized myogenic reporter genes. For this, we chose to analyze the myogenin promoter (*Myog-luc*) and the *Myod* promoter regions (*myod -2.5 kb/-275-luc*). In Fig. 3D, the ability of MyoD to activate its own promoter was repressed by TAZ S89A. In Fig. 3E, we document that TAZ S89A also inhibits the activation of the *Myog* promoter in myogenic cells, and we report a corresponding decrease in myogenin protein level with ectopic TAZ expression (Fig. 3F). Collectively, these data indicate that TAZ potently represses a number of myogenic promoters (*Ckm*, *Myog* and *Myod*), while still retaining its potent co-activator potential at a TEAD responsive reporter gene (HIP/HOP system). In view of the potent repression of a number of critical myogenic regulators in our assays, we questioned whether TAZ might influence the commitment to the myogenic lineage. To do this we utilized the well-characterized myogenic 'conversion assay' in which MyoD expression converts 10T1/2 fibroblasts into myogenic cells. We used fluorescently tagged MyoD (GFP–MyoD) and TAZ S89A (mCherry–TAZ S89A) to assess the transfected cells in this assay. As depicted in Fig. 3G, we observed that, as expected, MyoD (GFP tagged) 'converted' cells into multinucleated myotubes and mCherry alone had no effect on myogenic conversion (lower panel). Conversely, when GFP–MyoD was co-transfected with mCherry–TAZ S89A there was no myogenic conversion detected (upper panel). We also assessed MyoD-mediated myogenic conversion in this assay system by measuring the cell lengths, based on the logic that elongated multinucleated muscle cells have a considerably greater length than the parental 10T1/2 cells (Fig. 3G, graph). In this alternative myogenic model system, these data indicate that TAZ robustly suppresses myogenic

Journal of Cell Science (2022) 135, jcs259097. doi:10.1242/jcs.259097

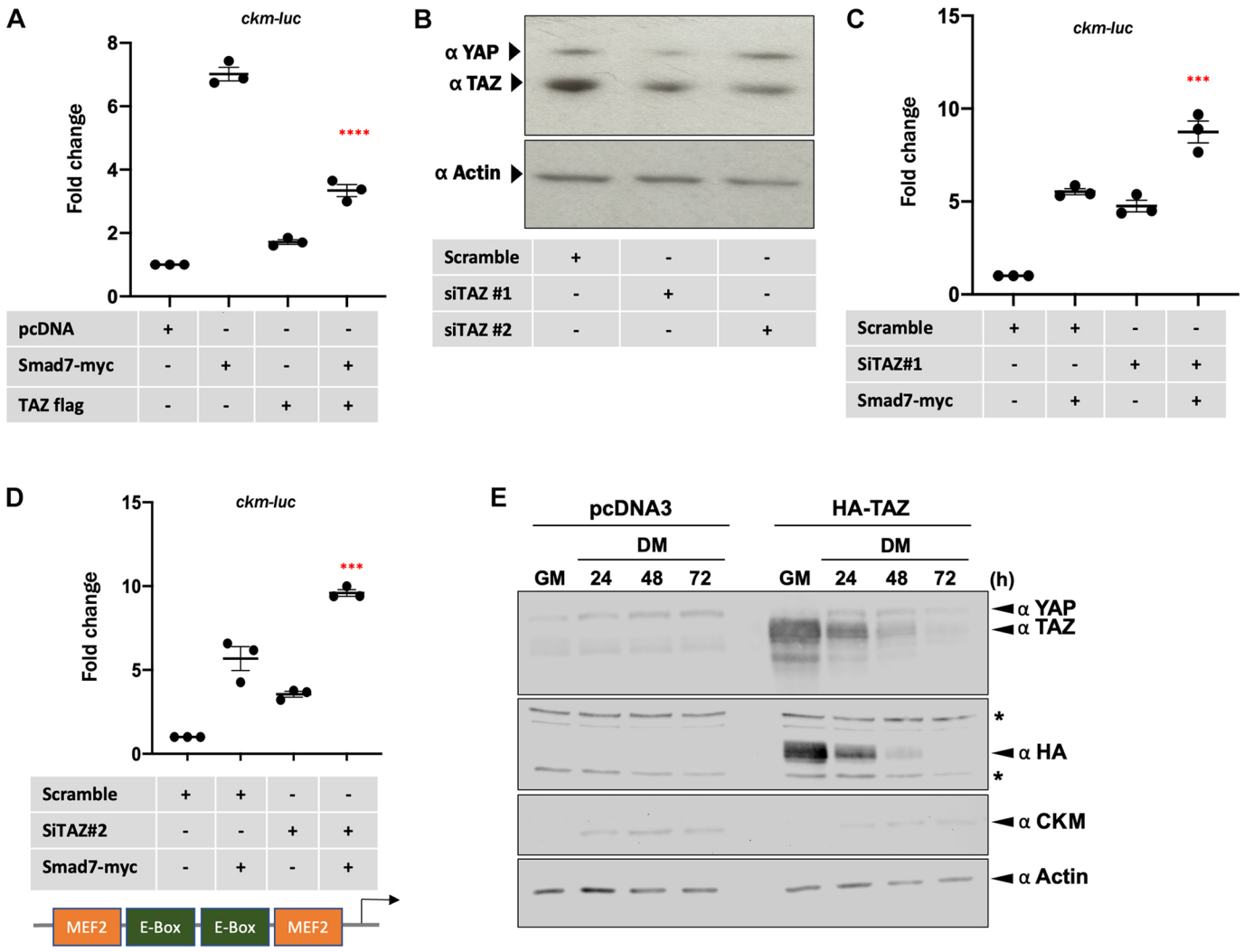

Fig. 2. TAZ inhibits the activity of Smad7 on the *Ckm* promoter. (A) Smad7–Myc and TAZ–Flag alone or in combination were ectopically expressed in C2C12 cells along with a *Ckm* luciferase reporter gene. *Renilla* served as transfection control. C2C12 transfected with empty vector (pcDNA) and indicated reporter genes served as controls for endogenous activity. Cells were harvested for luciferase determination at 48 h after changing to DM post-transfection. Normalized luciferase activity was compared to the control to determine fold changes. (B) Two siRNAs specific for TAZ were used to deplete the endogenous TAZ levels in C2C12. Unprogrammed Scrambled siRNA was used as control. (C,D) Smad7–Myc was transfected along with *Ckm* luciferase. *Renilla* was used as a control reporter to monitor and normalize for transfection efficiency. Lysates were collected at 48 h after changing to differentiation medium (DM) post-transfection. Firefly luciferase activity under each condition was measured independently and normalized to *Renilla* values. Each condition was compared to the control for the three individually transfected samples to determine fold change. Each bar represents the mean of three technical replicates. The error bars represent s.e.m. ***$P \leq 0.001$, ****$P < 0.0001$ compared to the relevant control condition (one-way ANOVA with Tukey's multiple comparisons test). (E) HA–TAZ and pcDNA3 control were ectopically expressed in C2C12 and grown for 24 h before switching to differentiation medium for 24 to 72 h. Lysates were collected and assessed for expression of TAZ, HA, CKM and actin by western blot analysis. Blot representative of one experiment.

conversion. As shown in Fig 3H,I, we observed that whereas MyoD and β-catenin have no effect on TAZ activity using the HIP/HOP reporter system, TAZ potently represses β-catenin activity on the β-catenin-dependent TOP flash reporter gene. These data consistently support the idea that TAZ has an asymmetric function as both a transcriptional activator and repressor depending on the enhancer/promoter element context.

Differential TAZ and YAP phosphorylation during skeletal muscle differentiation

Cell–cell contact has been identified as a regulator of Hippo signaling. Activation of Hippo signaling at high cell densities results in a well-characterized phosphorylation and cytoplasmic sequestration of TAZ at Ser89, promoting its binding to 14-3-3 proteins in the cytoplasm (Wada et al., 2011). Therefore, we were interested to determine the levels of endogenous Ser89 phosphorylated TAZ during myogenic differentiation. Time course analysis of total protein lysates from differentiating cells indicate that TAZ levels remain relatively unchanged during differentiation, although TAZ is much more abundant than YAP in muscle cells. Importantly, hyperphosphorylation of TAZ was pronounced when the cells were differentiating, suggesting activation of Hippo signaling in differentiation conditions (Fig. 4A,B). Immunofluorescence analysis of TAZ and phospho-TAZ also indicates that TAZ localization shifts from being predominantly nuclear during the myoblast stage (low cell density) to a more diffuse cytoplasmic localization in differentiating myotubes (high cell density), although some TAZ is still retained in the nucleus. Phosphorylated TAZ is undetectable in mononucleated myoblasts (Fig. 4C) and primarily localized in the cytoplasm in differentiated

Journal of Cell Science (2022) 135, jcs259097. doi:10.1242/jcs.259097

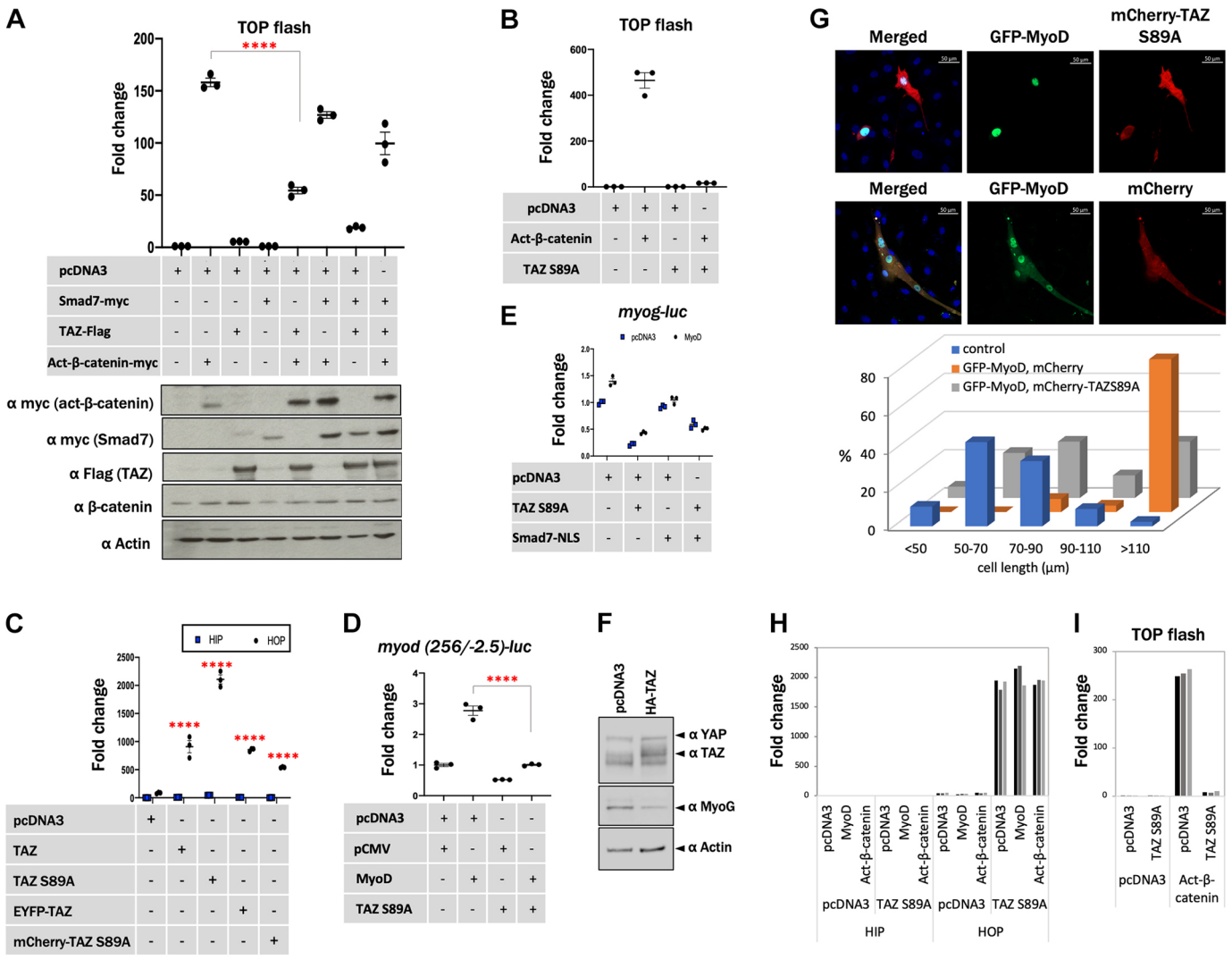

Fig. 3. TAZ inhibits β-catenin mediated *trans*activation properties. (A) Smad7–Myc, TAZ–Flag and β-catenin alone or in combination were ectopically expressed along with a TOP flash (FOP flash negative control data is in Fig. S1) luciferase reporter gene. *Renilla* luciferase served as transfection control. Transfection with empty vector (pcDNA) and reporter genes served as controls for endogenous activity. Cells were harvested for Luciferase determination at 16 h post transfection. Normalized luciferase activity was compared to the control to determine fold changes. Lower panels indicate western blot analysis of the protein levels derived from transfected plasmids. (B) Graph indicating the activity of TAZ S89A on β-catenin-mediated activation of TOP flash. (C) Graph documenting the transactivation properties of different TAZ expression constructs (wt TAZ, TAZ S89A, EYFP–TAZ, mCherry–ΔTAZ, and mCherry–TAZ S89A] on the HIP and HOP (HOP is driven by multimerized TEAD binding sites whereas HIP is the same reporter with mutated TEAD binding sites serving as a negative control) reporter gene system (see Materials and Methods for further details). (D,E) Graph showing the effect of TAZ S89A on the *Myod* (−2.5 *kb*/-275)-luc reporter gene or *Myog*-luc (E) reporter gene. Results show the activity of TAZ S89A and Smad7, alone or in combination, on the reporter. Each bar for A–E represents mean of three replicates. The error bars represent s.e.m. ****P<0.0001 (one-way ANOVA with Tukey's multiple comparisons test). (F) HA-TAZ and pcDNA3 control were ectopically expressed in C2C12 and grown for 24 h before collecting lysates and assessing for expression of TAZ, MyoG and actin by western blot analysis. Blot is representative of one experiment. (G) C310T1/2 cells were transfected for transient expression of the indicated constructs. One day after transfection, the cells were transferred to DM for 4 days for myotube formation. The cell morphology was recorded by live-cell confocal fluorescence microscopy. The length of the cells was measured by Zen software (control; untransfected; n=252, GFP–MyoD plus mCherry; n=29, GFP–MyoD plus mCherry–TAZ S89A; n=17) on the recorded micrograph. The percentage of cells in indicated length categories over total cell count were graphed. (H) MyoD or activated (Act)-β-catenin alone or in combination with TAZ S89A were ectopically expressed in C2C12 cells along with a HOP/HIP or (I) TOP flash reporter gene. *Renilla* served as transfection control. Cells were harvested for luciferase determination at 16 h post transfection. Normalized luciferase activity was compared to the control to determine fold changes. Results are means of triplicate data points in one experiment. Scale bars: 50 μm.

myotubes (Fig. 4D). Taken together, these observations are consistent with a model in which the nuclear function of TAZ predominates in proliferating myoblasts. However, under differentiation conditions, activation of Hippo signaling results in TAZ Ser89 phosphorylation and increased retention in the cytoplasm. Based on the repressive function of TAZ at the *Ckm* gene that we have documented here, we propose that TAZ represses myogenic transcription complexes under proliferative conditions, and activation of Hippo signaling during differentiation relieves this repression by the phospho-dependent sequestration of TAZ in the cytoplasm. Analysis of proliferating C2C12 cells by immunofluorescence suggested that TAZ forms a pattern of speckled localization, which can be indicative of phase separation properties (Fig. 4E). These initial observations of the localization of endogenous TAZ in muscle cells led us to speculate that TAZ might form phase condensates, and we therefore subsequently proceeded to test this possibility.

Journal of Cell Science (2022) 135, jcs259097. doi:10.1242/jcs.259097

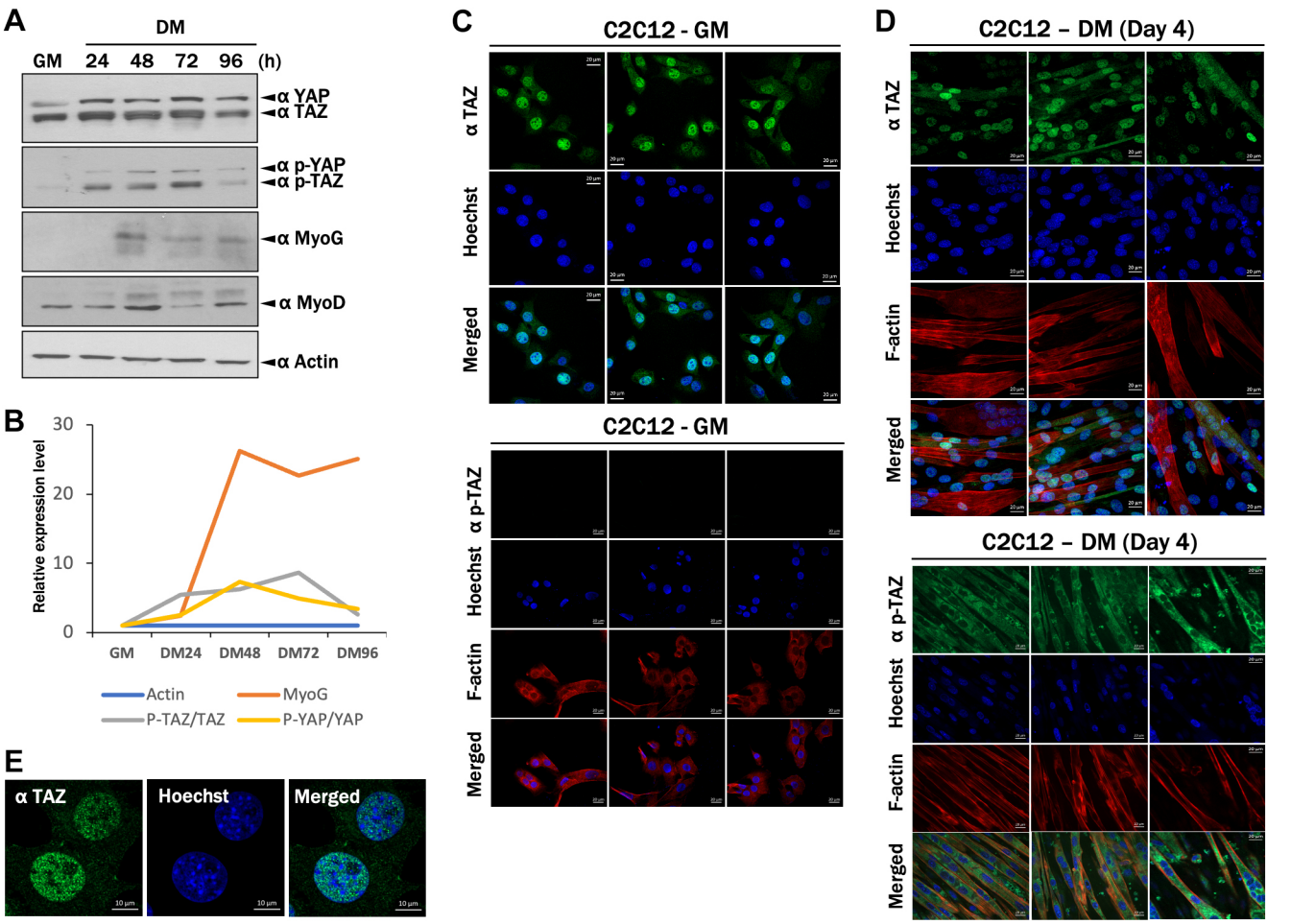

Fig. 4. TAZ is differentially phosphorylated and localized in proliferative and differentiating myogenic cells. (A) C2C12 myoblasts were cultured in growth medium (GM) for 24 h before transfer into differentiation medium (DM) for 24 to 96 h. Lysates were collected and assessed for expression of TAZ, phospho-TAZ and muscle markers by western blot analysis. Blot representative of one experiment. (B) The relative expression level of indicated proteins (from A) was estimated by measuring the band intensity corresponding to the protein captured on the film using ImageJ. Relative intensity of the bands was initially standardized to the actin loading control at each time point. To establish the relative level of phosphorylation, the ratio of the phosphorylated to total protein was calculated and plotted. Results are representation of A. (C,D) Immunofluorescence analysis of endogenous TAZ and phospho-TAZ during myoblast (GM) and myotube (DM day 4) conditions. Staining with Hoechst 33342 and F-actin indicate nuclei and myotubes, respectively. (E) At higher magnification, TAZ immunofluorescence exhibits a nuclear speckle pattern in GM conditions. The images in the time course (C,D) were from one experiment. The images in E are representative of staining pattern in one experiment. Scale bars: 20 µm (C,D); 10 µm (E).

TAZ exhibits robust phase separation properties in muscle cells

Liquid–liquid phase separation (LLPS) of proteins and nucleic acids into condensates (also referred to as nuclear speckles, nuclear bodies or biomolecular condensates) is invoked by weak multivalent interactions between molecules (Banani et al., 2017; Shin and Brangwynne, 2017). Phase separation has recently been implicated in heterochromatin domain formation (Larson et al., 2017; Strom et al., 2017), transcriptional control through co-activator condensation (Boija et al., 2018; Sabari et al., 2018), and the clustering of nuclear enhancer elements and super-enhancers in gene control (Hnisz et al., 2017). Our observations indicate that TAZ displays a number of properties associated with phase separation that may underlie its diverse activities in both activation and repression of gene regulation.

As observed in fluorescence live-cell imaging analysis, ectopically expressed EYFP–TAZ wild-type (WT) and EYFP-TAZ S89A (nuclear TAZ) formed a similar localization pattern of spherical structures in the nucleus (Fig. 5A; Movies 1 and 2). Ectopic EYFP-tagged TAZ expression therefore allowed us to perform more detailed and higher resolution analysis of the TAZ nuclear speckles. Both EYFP–TAZ (WT) and EYFP–TAZ S89A formed dynamic spherical subcellular structures. We further observed that TAZ condensates were, in some cases, juxtaposed with heterochromatin, with projections extending into the heterochromatin domain (Fig. 5A; Movie 1). Conversely, we also noted patterns of localization within the same nuclei in which the TAZ condensates are not associated with heterochromatin. These differential associations may therefore reflect variant TAZ-containing complexes involved in gene activation or repression. Furthermore, fusion of the spherical structures was observed in time-lapse live-cell imaging analysis (Fig. 5B; Movie 2). These observations of the robust capability of TAZ to form condensates was recently reported under *in vitro* conditions and also in cultured MCF-10A cells (Franklin and Guan, 2020). In addition, YAP has also been shown to exhibit LLPS (Cai et al., 2019; Yu et al., 2021).

Next, we assessed whether β-catenin might also be localized in these phase-separated condensates with TAZ and Fig. 5C depicts that it is. We observed two types of phase condensates in these experiments. There was a TAZ-negative central region in the center

Journal of Cell Science (2022) 135, jcs259097. doi:10.1242/jcs.259097

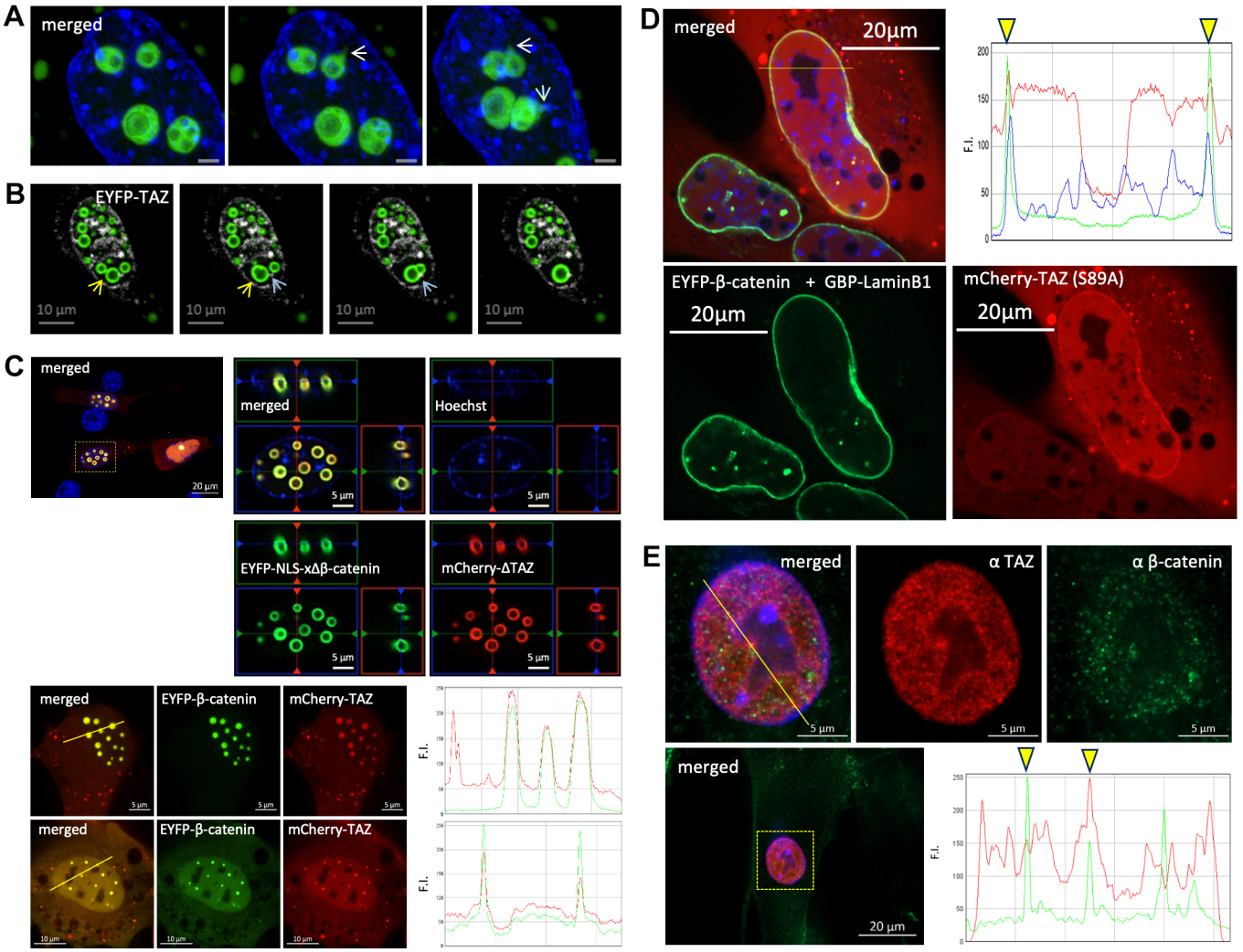

Fig. 5. TAZ exhibits robust phase separation properties in myogenic cells. (A,B) Live-cell spinning disc confocal imaging of ectopically expressed EYFP–TAZ indicates spherical condensate structures, B indicates fusion properties of EYFP-TAZ condensates. Time-lapse demonstration of nuclear condensate formation and fusion of EYFP-TAZ by live-cell imaging (see Movies 1 and 2). Arrows indicate separate fusion events of EYFP–TAZ foci depicted in Movies 1 and 2. (C) C2C12 cells were transfected with indicated expression constructs. After 1 day, the cells were subjected to live-cell confocal fluorescence microscopy. Orthogonal projection micrographs rendered from *Z*-stack images (240 nm interval) show *XY*-, *XZ*-, and *YZ*-optical planes. The micrograph of lower expression samples were also analyzed for colocalization by line-scan analysis for fluorescence intensity (F.I.) of green (EYFP–β-catenin) and red (mCherry–TAZ) and plotted by ImageJ. (more analyses are in Fig. S3). (D) C2C12 cells were transfected with indicated expression constructs. After 1 day, the cells were subjected to live-cell confocal fluorescence microscopy. EYFP–β-catenin was localized to the nuclear envelope by an interaction trap using GBP–LaminB1. A line scan analysis along the indicated yellow line in the merged micrograph depicts recruitment of mCherry-TAZ to the EYFP-β-catenin trapped at the nuclear envelope, as indicated by arrowheads (more analyses are in Fig. S4). (E) C2C12 cells in DM for 4 days were fixed and subjected to IF analysis for endogenous TAZ and β-catenin. Colocalization of TAZ and β-catenin nuclear speckles were analyzed by line scan for fluorescent intensity by ImageJ. Data in Fig. 5 is representative of three separate experiments. Scale bars: 2 µm (A), 10 µm (B), 20 µm (C,E, overview image); 5 µm (C,E, magnified images).

of some spherical condensates (Fig. 5C, upper panels) while in others then whole condensate was TAZ positive (Fig. 5C, lower panels). At this point we cannot determine whether this is related to the expression level or the state of maturation of the TAZ condensates. To further test how robust this protein–protein interaction is, we used a nanotrap assay to capture EYFP–β-catenin at the interior of nuclear envelope using GBP–Lamin B1 as the tether. Fig. 5D indicates that this approach was successful in re-directing β-catenin to the nuclear envelope. Strikingly, mCherry–TAZ S89A was subsequently enriched at the nuclear envelope due to its robust protein interaction with β-catenin (Fig. 5D; see Fig. S4 for additional images). Finally, some endogenous TAZ and β-catenin foci were colocalized in the nuclei of mononucleated myogenic reserve cells, as revealed by immunofluorescence analysis (Fig. 5E). Collectively, these features of TAZ and β-catenin localization and dynamic assembly into condensates are consistent with LLPS properties recently reported for YAP, TAZ and other nuclear regulatory proteins (Boeynaems et al., 2018; Boija et al., 2018; Hnisz et al., 2017; Sabari et al., 2018).

DISCUSSION

The Hippo pathway has garnered widespread attention for its role in both physiological and pathological conditions in a variety of tissues. It has now been implicated in organ growth and development, stem cell biology, regeneration and tumorigenesis (Moroishi et al., 2015; Piccolo et al., 2014; Yu et al., 2015). The Hippo pathway is composed of a core kinase module and a

Journal of Cell Science (2022) 135, jcs259097. doi:10.1242/jcs.259097

transcriptional regulatory complex comprised of TAZ and/or YAP as the main effectors. To date, many cellular studies have documented how TAZ and YAP phosphorylation and nuclear localization are controlled. More recently, there have been efforts to reveal regulatory mechanisms governing how YAP and TAZ can exert selective functions on the transcriptional apparatus assembled at different *cis*-regulatory elements in the genome (Totaro et al., 2018). In this study, we document how nuclear TAZ inhibits myogenic differentiation by repressing components of a well-characterized muscle-specific transcription complex.

In particular, we characterize components of a pro-myogenic protein complex comprising Smad7 and β-catenin that is antagonized by TAZ protein interactions, thus serving to suppress transcriptional activation of muscle-specific genes, maintaining the cells in an undifferentiated, proliferative state. These data support a model for nuclear TAZ function in suppressing the myogenic differentiation program by targeting a key transcriptional regulatory complex assembled on muscle promoters. Phosphorylation-dependent cytoplasmic sequestration of TAZ by activation of Hippo kinases relieves this repression, providing a potential switch to allow the myogenic differentiation program to proceed. Interestingly, as reported by others recently (Lu et al., 2020), we observe TAZ in myonuclear speckles consistent with key features of phase-separated condensates, including high sphericity and fusion behavior. These studies outline a functional reciprocity between myogenic differentiation and Hippo signaling that may have important implications for our understanding of the co-ordination of cellular proliferation and differentiation in skeletal muscle growth control.

While YAP and TAZ are often considered functionally redundant, there are structural and functional observations indicating that they might also have non-overlapping roles (Plouffe et al., 2018). Despite their high sequence similarity, there are nevertheless some potentially important differences in their structure. Notably, although both proteins contain WW domains, YAP harbors two tandem WW domains, whereas TAZ has one. Also, YAP contains an SH3 binding domain, which is not present in TAZ. Of some interest for our study, in view of the TAZ connection with β-catenin, is the reported observation that GSK3β, a well-characterized regulator of β-catenin, can directly phosphorylate TAZ affecting its stability. Several reports in different model systems indicate that TAZ cannot compensate for YAP physiologically, supporting the idea that, while they are both targets of the Hippo kinase pathway, they also retain distinct roles (Hossain et al., 2007; Makita et al., 2008; Morin-Kensicki et al., 2006).

Given the structural and physiological differences between YAP and TAZ it is possible that their interactions with transcriptional complexes may differ. This is particularly highlighted in recent studies documenting differential properties of YAP and TAZ in promoting the formation of LLPS with different factors being sequestered within the condensates (Lu et al., 2020; Cai et al., 2019). It is now becoming increasingly apparent that the subcellular assemblage of membrane-less compartments through LLPS is an essential feature of temporal and spatial control of various biomolecular processes (Boeynaems et al., 2018; Boija et al., 2018; Cai et al., 2019; Hyman et al., 2014; Lu et al., 2019; Sabari et al., 2018). Here, we confirm and extend these observations in reporting that TAZ forms liquid–liquid phase-like condensates in cultured muscle cells. Moreover, hyperosmotic stress promotes the rapid assembly and fusion of spherical TAZ condensates leading to the compartmentalization of TAZ and its interacting partners. Our observations confirm a recent report documenting that TAZ forms liquid-like condensates that concentrate transcriptional regulatory proteins such as co-activators and the elongation machinery (Lu et al., 2020). One of the primary cellular functions of Hippo signaling is to control tissue growth by regulating the proliferative expansion of progenitor pools. Based on our data, we speculate that TAZ nuclear condensates sequester components of the myogenic nuclear machinery involved in cellular differentiation. Thus, TAZ-mediated 'hijacking' and repression of the pro-differentiation machinery might be deemed complementary to its pro-proliferative activities underlying growth. A pro-proliferative role of TAZ in muscle satellite cells was reported in a previous study employing an *in vivo* strategy in satellite cells (Sun et al., 2017), which is consistent with our observations; however, that study also proposed a pro-differentiation effect of TAZ in the later stages of differentiation, which is not congruent with our observations in myoblasts. This could potentially be explained by the enhanced 'early' proliferation promoted by YAP and TAZ leading to an enhanced accumulation of progenitors and a more robust eventual differentiated phenotype *in vivo*. We would also contend that this might be further complicated by the potential for Hippo pathway activation in the *in vivo* context, which would lead to TAZ cytoplasmic retention, and thus sequestration away from the differentiation machinery due to activation of Hippo kinases when the cells eventually commit to the differentiation program. This would be consistent with our observations, since we expect that the repressive effect of TAZ on the differentiation machinery would only be operative under growth/proliferative conditions. It will be interesting to further assess and clarify these possibilities regarding the physiological role of TAZ in different muscle contexts in future.

The best-characterized partners for YAP and TAZ in transcriptional control are the TEAD1–TEAD4 factors, although to date the possibility of different partners for YAP and TAZ has not been exhaustively tested. Of particular relevance for the discussion of muscle transcription complexes is the previously reported interaction of TEAD factors with the MEF2 proteins, which are core regulators of the muscle transcription program (Chen et al., 2017; Maeda et al., 2002). It is perhaps coincidental, but noted, that p38 MAPKs are a potent and well-characterized regulator of MEF2 function, and it was recently documented that TEAD function is also targeted by p38 MAPKs (Lin et al., 2017). Moreover, our recent studies have documented an interaction between MEF2 and β-catenin that is p38 MAPK dependent (Ehyai et al., 2016), and a direct physical interaction between β-catenin and Smad7 (Tripathi et al., 2019), in a muscle context. Thus, the TAZ–Smad7 interaction reported here may intersect with these protein interactions. The schematic in Fig. 6 documents a working model of these interactions. Collectively, these observations support a model in which a core muscle transcriptional regulatory complex may be targeted by ancillary regulatory subunits, such as TAZ or β-catenin–Smad7, to repress or enhance its activity, respectively, depending on the cellular conditions. Collectively, these observations place TAZ in the cellular context of muscle-specific gene regulation. It will be of considerable interest to further examine the physiological role of TAZ in post-natal muscle growth and regeneration in health and disease.

MATERIALS AND METHODS

Cell culture

C2C12 myoblasts and C3H10T1/2 cells were obtained from the American Type Culture Collection. Cells were cultured in growth medium (GM) consisting of high-glucose Dulbecco's modified Eagle's medium

Journal of Cell Science (2022) 135, jcs259097. doi:10.1242/jcs.259097

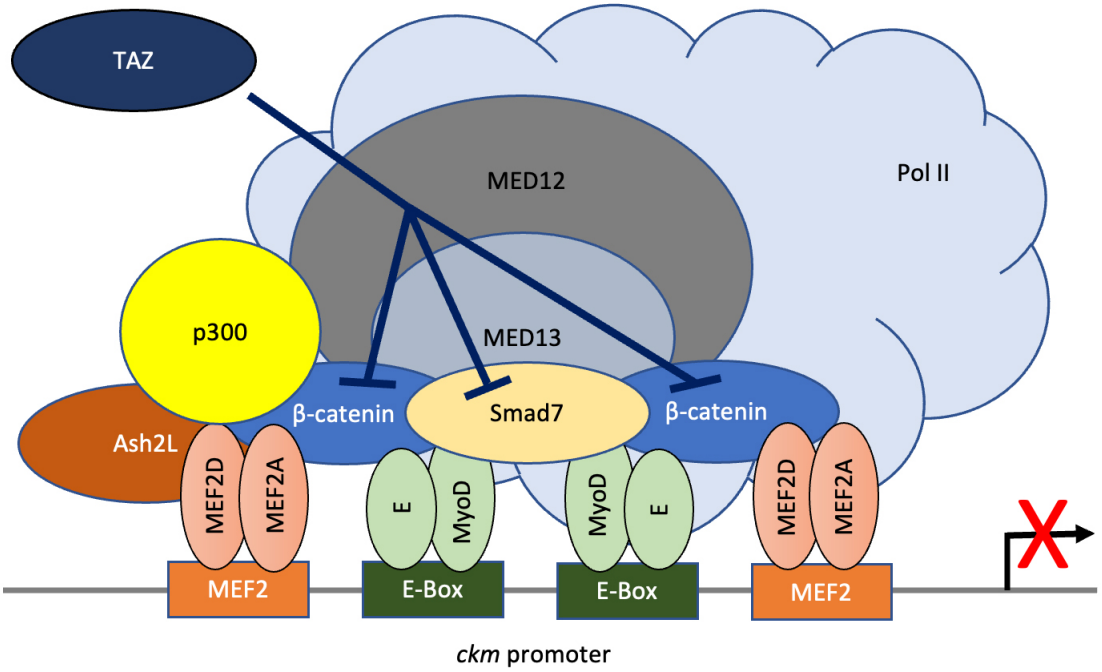

Fig. 6. A schematic view of a myogenic 'holocomplex' highlighting TAZ function. Based on extensive previous reports in the literature and our own publications, this schematic represents the assembly of a generic myogenic 'holocomplex' on muscle specific promoters. We have added TAZ as an accessory factor to this schematic to indicate its potential role, based on data included herein. E refers to E12/E47 proteins. See Discussion for further detail.

(DMEM, Gibco), 10% fetal bovine serum (FBS) and L-Glutamine (HyClone) supplemented with 1% penicillin-streptomycin (Invitrogen, Thermo Fisher Scientific). Myotube formation was induced by replacing GM with differentiation medium (DM), consisting of DMEM supplemented with 2% horse serum (Atlanta Biologicals) and 1% penicillin-streptomycin. Cells were maintained in an incubator at 95% humidity, 5% CO_2 and 37°C.

Transfections

For ectopic protein expression, cells were transfected using the calcium phosphate precipitation method for transcription reporter assays. Cells were re-fed 16 h post-transfection and harvested. For small interfering RNA (siRNA) experiments, C2C12 myoblasts were transfected with Lipofectamine 2000 (Life Technologies) using instructions provided by the manufacturer and harvested 48 h later, unless otherwise indicated.

Gene silencing

Knockdown of target genes was done using mission siRNA (Sigma-Aldrich). siTAZ#1 (SASI Mm01 00107364) and siTAZ#2 (SASI Mm01 00107368) and universal scrambled siRNA (SIC001) were used at 50 nM concentrations.

Plasmids

Expression plasmids for Myc-His-tagged full-length Smad7, FLAG-TAZ, β-catenin-Myc, transcription reporter assay constructs *Ckm-luc* and TOP/FOP flash have been described previously (Ehyai et al., 2016; Kollias et al., 2006; Miyake et al., 2010; Pagiatakis et al., 2017). HIP-Flash (#83466) and HOP-flash (#83467) were obtained from Addgene (Kim and Gumbiner, 2015). mCherry/EYFP tagged TAZ and β-catenin constructs were described previously (Ehyai et al., 2018; Pagiatakis et al., 2017). *Myod* (-2.5/-275)-luc was a kind gift from Dr Steven Tapscott, Fred Hutchinson Cancer Research Center (Seattle, USA) (Asakura et al., 1995). *Myog*-luc was described previously (Miyake et al., 2010).

Transcription reporter gene assays

Transcriptional reporter assays were performed using luciferase reporter plasmids along with expression constructs (indicated in figure legends) and a *Renilla* plasmid (pRL-*Renilla*, Promega) as an internal control. Cells were washed with 1× PBS and harvested in luciferase lysis buffer (20 mM Tris-HCl pH 7.4 and 0.1% Triton X-100). Enzymatic activity was measured in each sample on a luminometer (Lumat LB, Berthold) using luciferase assay substrate (E1501; Promega) or *Renilla* assay substrate (E2820; Promega). Luciferase activity values obtained were normalized to *Renilla* activity in the same cell extracts and expressed as fold activation to the control.

Western blotting

Total cellular protein extracts were prepared in NP-40 lysis buffer [0.5% NP40 (v/v), 50 mM Tris-HCl pH 8, 150 mM NaCl, 10 mM sodium pyrophosphate, 1 mM EDTA pH 8, and 0.1 M NaF supplemented with 1× protease inhibitor cocktail (P-8340; Sigma) and 0.5 mM sodium orthovanadate]. Protein concentrations were determined by a standard Bradford assay. Equivalent amounts of protein were denatured in SDS loading buffer at 100°C for 5 min and then run in SDS-polyacrylamide gels, followed by electrophoretic transfer onto Immobilon-FL PVDF membrane (Millipore) as directed by the manufacturer. Blots were incubated with blocking buffer that consisted of 5% milk in Tris-buffered saline with Tween 20 (TBS-T; 10 mM Tris-HCl, pH 8.0, 150 mM NaCl, 0.1% Tween 20) prior to the incubation with primary antibody (please see below for the dilution of each antibody) at 4°C overnight with gentle agitation. After three washes with TBS-T, appropriate HRP-conjugated secondary antibodies (BioRad, 1:2000), were added for 2 h at room temperature. Protein–antibody immuno-complexes were detected with enhanced chemiluminescence western blotting substrate (Pierce, ThermoFisher).

Antibodies

Rabbit monoclonal for TAZ (mAb8418, 1:1000), phospho-TAZ (mAb59971, 1:1000) and β-catenin (pAb9562, 1:2000) were purchased from Cell Signaling. Monoclonal anti-Flag antibody (F1804, 1:1000) was from Sigma. Antibodies against Myc (9E10, 1:20), HA (12CA5, 1:20), MyHC (MF20, 1:20) and myogenin (F5D, 1:20) were purchased from DSHB. Antibodies against Actin (I-19; sc-1616, 1:1000), MyoD (C-20; sc-304, 1:2000), and CKM (G-9; sc-365046, 1:200) were purchased from Santa Cruz Biotechnology.

Co-immunoprecipitation

For co-immunoprecipitation assays (co-IP), C2C12 myoblasts were transfected with Flag-tagged Smad7 or Trim28 using Lipofectamine 2000. Cells were re-fed 16 h post-transfection and total protein lysates were harvested 24 h after the medium change. Proteins were extracted as described above. Immunoprecipitation was performed using anti-Flag M2 magnetic beads (Sigma, M8823) according to the manufacturer's instructions. Eluates were analyzed by western blotting as described above.

Immunofluorescence analysis

C2C12 cells were seeded on the glass-bottom dishes (MatTek) and fixed with 4% PFA. Cells were washed (three times) with 1× PBS and permeabilized with ice cold 90% Me-OH for 1 min. Cells were washed again (three times) with 1× PBS and incubated with blocking buffer (5% FBS in 1× PBS) for 2 h at room temperature, and then incubated with an indicated primary antibody in the blocking buffer overnight at 4°C. After removal of the unbound primary antibody, the cells were incubated with Alexa Fluor-conjugated secondary antibody (Life Technologies) in the blocking buffer at room temperature for 1.5 h. After washing with 1× PBS three times, the cells were subjected to imaging with a Zeiss Observer Z1 confocal fluorescent microscope equipped with Yokogawa CSU-X1 spinning disk. Images were recorded by AxioCam MRm camera (Zeiss) and processed by Zen 2.5 (blue edition) software (Zeiss).

Live-cell imaging

C2C12 cells were seeded on polymer-coated glass-bottom dishes (#81158, ibidi). The cells were transfected with expression plasmids encoding the indicated fluorescently tagged proteins. The cell culture media was exchanged for FluoBrite (A1896701, ThermoFisher) with 10% FBS (HyClone). The cells were maintained in a moisturized environmental chamber (5% CO2) on the Zeiss Observer Z1 confocal fluorescent microscope platform during live cell imaging.

Competing interests

The authors declare no competing or financial interests.

Author contributions

Conceptualization: S.T., T.M., J.C.M.; Methodology: S.T., T.M., J.C.M.; Validation: T.M., J.C.M.; Formal analysis: S.T., T.M.; Investigation: S.T., T.M., J.K.; Resources: J.C.M.; Data curation: J.K.; Writing - original draft: S.T., T.M., J.K., J.C.M.; Writing - review & editing: T.M., J.K., J.C.M.; Visualization: S.T., T.M.; Supervision: J.C.M.; Project administration: J.C.M.; Funding acquisition: J.C.M.

Funding

Work in the manuscript was funded by a project grant from Canadian Institute of Health Research (CIHR) to J.C.M. (PJT-159644). S.T. was funded by a Millennium Scholarship from the Ontario Government.

Peer review history

The peer review history is available online at https://journals.biologists.com/jcs/article-lookup/doi/10.1242/jcs.259097.

References

Alarcon, C., Zaromytidou, A. I., Xi, Q., Gao, S., Yu, J., Fujisawa, S., Barlas, A., Miller, A. N., Manova-Todorova, K., Macias, M. J. et al. (2009). Nuclear CDKs drive Smad transcriptional activation and turnover in BMP and TGF-beta pathways. *Cell* **139**, 757-769. doi:10.1016/j.cell.2009.09.035

Anand, M., Lai, R. and Gelebart, P. (2011). beta-catenin is constitutively active and increases STAT3 expression/activation in anaplastic lymphoma kinase-positive anaplastic large cell lymphoma. *Haematologica* **96**, 253-261. doi:10.3324/haematol.2010.027086

Asakura, A., Lyons, G. E. and Tapscott, S. J. (1995). The regulation of MyoD gene expression: conserved elements mediate expression in embryonic axial muscle. *Dev. Biol.* **171**, 386-398. doi:10.1006/dbio.1995.1290

Azzolin, L., Zanconato, F., Bresolin, S., Forcato, M., Basso, G., Bicciato, S., Cordenonsi, M. and Piccolo, S. (2012). Role of TAZ as mediator of Wnt signaling. *Cell* **151**, 1443-1456. doi:10.1016/j.cell.2012.11.027

Azzolin, L., Panciera, T., Soligo, S., Enzo, E., Bicciato, S., Dupont, S., Bresolin, S., Frasson, C., Basso, G., Guzzardo, V. et al. (2014). YAP/TAZ incorporation in the beta-catenin destruction complex orchestrates the Wnt response. *Cell* **158**, 157-170. doi:10.1016/j.cell.2014.06.013

Banani, S. F., Lee, H. O., Hyman, A. A. and Rosen, M. K. (2017). Biomolecular condensates: organizers of cellular biochemistry. *Nat. Rev. Mol. Cell Biol.* **18**, 285-298. doi:10.1038/nrm.2017.7

Boeynaems, S., Alberti, S., Fawzi, N. L., Mittag, T., Polymenidou, M., Rousseau, F., Schymkowitz, J., Shorter, J., Wolozin, B., Van Den Bosch, L. et al. (2018). Protein phase separation: a new phase in cell biology. *Trends Cell Biol.* **28**, 420-435. doi:10.1016/j.tcb.2018.02.004

Boija, A., Klein, I. A., Sabari, B. R., Dall'Agnese, A., Coffey, E. L., Zamudio, A. V., Li, C. H., Shrinivas, K., Manteiga, J. C., Hannett, N. M. et al. (2018). Transcription factors activate genes through the phase-separation capacity of their activation domains. *Cell* **175**, 1842-1855.e16. doi:10.1016/j.cell.2018.10.042

Cai, D., Feliciano, D., Dong, P., Flores, E., Gruebele, M., Porat-Shliom, N., Sukenik, S., Liu, Z. and Lippincott-Schwartz, J. (2019). Phase separation of YAP reorganizes genome topology for long-term YAP target gene expression. *Nat. Cell Biol.* **21**, 1578-1589. doi:10.1038/s41556-019-0433-z

Chen, X., Gao, B., Ponnusamy, M., Lin, Z. and Liu, J. (2017). MEF2 signaling and human diseases. *Oncotarget* **8**, 112152-112165. doi:10.18632/oncotarget.22899

Cohen, T. V., Kollias, H. D., Liu, N., Ward, C. W. and Wagner, K. R. (2015). Genetic disruption of Smad7 impairs skeletal muscle growth and regeneration. *J. Physiol.* **593**, 2479-2497. doi:10.1113/JP270201

Ehyai, S., Dionyssiou, M. G., Gordon, J. W., Williams, D., Siu, K. W. and McDermott, J. C. (2016). A p38 Mitogen-activated protein kinase-regulated myocyte enhancer factor 2-beta-catenin interaction enhances canonical Wnt signaling. *Mol. Cell. Biol.* **36**, 330-346. doi:10.1128/MCB.00832-15

Ehyai, S., Miyake, T., Williams, D., Vinayak, J., Bayfield, M. A. and McDermott, J. C. (2018). FMRP recruitment of beta-catenin to the translation pre-initiation complex represses translation. *EMBO Rep.* **19**, e45536. doi:10.15252/embr.201745536

Ferrigno, O., Lallemand, F., Verrecchia, F., L'Hoste, S., Camonis, J., Atfi, A. and Mauviel, A. (2002). Yes-associated protein (YAP65) interacts with Smad7 and potentiates its inhibitory activity against TGF-beta/Smad signaling. *Oncogene* **21**, 4879-4884. doi:10.1038/sj.onc.1205623

Franklin, J. M. and Guan, K. L. (2020). YAP/TAZ phase separation for transcription. *Nat. Cell Biol.* **22**, 357-358. doi:10.1038/s41556-020-0498-8

Hnisz, D., Shrinivas, K., Young, R. A., Chakraborty, A. K. and Sharp, P. A. (2017). A phase separation model for transcriptional control. *Cell* **169**, 13-23. doi:10.1016/j.cell.2017.02.007

Hossain, Z., Ali, S. M., Ko, H. L., Xu, J., Ng, C. P., Guo, K., Qi, Z., Ponniah, S., Hong, W. and Hunziker, W. (2007). Glomerulocystic kidney disease in mice with a targeted inactivation of Wwtr1. *Proc. Natl. Acad. Sci. USA* **104**, 1631-1636. doi:10.1073/pnas.0605266104

Huang, J., Wu, S., Barrera, J., Matthews, K. and Pan, D. (2005). The Hippo signaling pathway coordinately regulates cell proliferation and apoptosis by inactivating Yorkie, the Drosophila homolog of YAP. *Cell* **122**, 421-434. doi:10.1016/j.cell.2005.06.007

Huraskin, D., Eiber, N., Reichel, M., Zidek, L. M., Kravic, B., Bernkopf, D., von Maltzahn, J., Behrens, J. and Hashemolhosseini, S. (2016). Wnt/beta-catenin signaling via Axin2 is required for myogenesis and, together with YAP/Taz and Tead1, active in IIa/IIx muscle fibers. *Development* **143**, 3128-3142. doi:10.1242/dev.139907

Hyman, A. A., Weber, C. A. and Julicher, F. (2014). Liquid-liquid phase separation in biology. *Annu. Rev. Cell Dev. Biol.* **30**, 39-58. doi:10.1146/annurev-cellbio-100913-013325

Jia, J., Zhang, W., Wang, B., Trinko, R. and Jiang, J. (2003). The Drosophila Ste20 family kinase dMST functions as a tumor suppressor by restricting cell proliferation and promoting apoptosis. *Genes Dev.* **17**, 2514-2519. doi:10.1101/gad.1134003

Justice, R. W., Zilian, O., Woods, D. F., Noll, M. and Bryant, P. J. (1995). The Drosophila tumor suppressor gene warts encodes a homolog of human myotonic dystrophy kinase and is required for the control of cell shape and proliferation. *Genes Dev.* **9**, 534-546. doi:10.1101/gad.9.5.534

Kanai, F., Marignani, P. A., Sarbassova, D., Yagi, R., Hall, R. A., Donowitz, M., Hisaminato, A., Fujiwara, T., Ito, Y., Cantley, L. C. et al. (2000). TAZ: a novel transcriptional co-activator regulated by interactions with 14-3-3 and PDZ domain proteins. *EMBO J.* **19**, 6778-6791. doi:10.1093/emboj/19.24.6778

Kim, N. G. and Gumbiner, B. M. (2015). Adhesion to fibronectin regulates Hippo signaling via the FAK-Src-PI3K pathway. *J. Cell Biol.* **210**, 503-515. doi:10.1083/jcb.201501025

Kollias, H. D., Perry, R. L., Miyake, T., Aziz, A. and McDermott, J. C. (2006). Smad7 promotes and enhances skeletal muscle differentiation. *Mol. Cell. Biol.* **26**, 6248-6260. doi:10.1128/MCB.00384-06

Larson, A. G., Elnatan, D., Keenen, M. M., Trnka, M. J., Johnston, J. B., Burlingame, A. L., Agard, D. A., Redding, S. and Narlikar, G. J. (2017). Liquid droplet formation by HP1alpha suggests a role for phase separation in heterochromatin. *Nature* **547**, 236-240. doi:10.1038/nature22822

Lin, K. C., Moroishi, T., Meng, Z., Jeong, H. S., Plouffe, S. W., Sekido, Y., Han, J., Park, H. W. and Guan, K.-L. (2017). Regulation of Hippo pathway transcription factor TEAD by p38 MAPK-induced cytoplasmic translocation. *Nat. Cell Biol.* **19**, 996-1002. doi:10.1038/ncb3581

Lu, H., Liu, R. and Zhou, Q. (2019). Balanced between order and disorder: a new phase in transcription elongation control and beyond. *Transcription* **10**, 157-163. doi:10.1080/21541264.2019.1570812

Lu, Y., Wu, T., Gutman, O., Lu, H., Zhou, Q., Henis, Y. I. and Luo, K. (2020). Phase separation of TAZ compartmentalizes the transcription machinery to promote gene expression. *Nat. Cell Biol.* **22**, 453-464. doi:10.1038/s41556-020-0485-0

Maeda, T., Gupta, M. P. and Stewart, A. F. (2002). TEF-1 and MEF2 transcription factors interact to regulate muscle-specific promoters. *Biochem. Biophys. Res. Commun.* **294**, 791-797. doi:10.1016/S0006-291X(02)00556-9

Makita, R., Uchijima, Y., Nishiyama, K., Amano, T., Chen, Q., Takeuchi, T., Mitani, A., Nagase, T., Yatomi, Y., Aburatani, H. et al. (2008). Multiple renal cysts, urinary concentration defects, and pulmonary emphysematous changes in mice lacking TAZ. *Am. J. Physiol. Renal. Physiol.* **294**, F542-F553. doi:10.1152/ajprenal.00201.2007

Miyake, T., Alli, N. S. and McDermott, J. C. (2010). Nuclear function of Smad7 promotes myogenesis. *Mol. Cell. Biol.* **30**, 722-735. doi:10.1128/MCB.01005-09

Morin-Kensicki, E. M., Boone, B. N., Howell, M., Stonebraker, J. R., Teed, J., Alb, J. G., Magnuson, T. R., O'Neal, W. and Milgram, S. L. (2006). Defects in yolk sac vasculogenesis, chorioallantoic fusion, and embryonic axis elongation in mice with targeted disruption of Yap65. *Mol. Cell. Biol.* **26**, 77-87. doi:10.1128/MCB.26.1.77-87.2006

Moroishi, T., Hansen, C. G. and Guan, K. L. (2015). The emerging roles of YAP and TAZ in cancer. *Nat. Rev. Cancer* **15**, 73-79. doi:10.1038/nrc3876

Oh, H. and Irvine, K. D. (2011). Cooperative regulation of growth by Yorkie and Mad through bantam. *Dev. Cell* **20**, 109-122. doi:10.1016/j.devcel.2010.12.002

Pagiatakis, C., Sun, D., Tobin, S. W., Miyake, T. and McDermott, J. C. (2017). TGFbeta-TAZ/SRF signalling regulates vascular smooth muscle cell differentiation. *FEBS J.* **284**, 1644-1656. doi:10.1111/febs.14070

Pantalacci, S., Tapon, N. and Leopold, P. (2003). The Salvador partner Hippo promotes apoptosis and cell-cycle exit in Drosophila. *Nat. Cell Biol.* **5**, 921-927. doi:10.1038/ncb1051

Piccolo, S., Dupont, S. and Cordenonsi, M. (2014). The biology of YAP/TAZ: hippo signaling and beyond. *Physiol. Rev.* **94**, 1287-1312. doi:10.1152/physrev.00005.2014

Plouffe, S. W., Lin, K. C., Moore, J. L., III, Tan, F. E., Ma, S., Ye, Z., Qiu, Y., Ren, B. and Guan, K. L. (2018). The Hippo pathway effector proteins YAP and TAZ have both distinct and overlapping functions in the cell. *J. Biol. Chem.* **293**, 11230-11240. doi:10.1074/jbc.RA118.002715

Rampalli, S., Li, L., Mak, E., Ge, K., Brand, M., Tapscott, S. J. and Dilworth, F. J. (2007). p38 MAPK signaling regulates recruitment of Ash2L-containing methyltransferase complexes to specific genes during differentiation. *Nat. Struct. Mol. Biol.* **14**, 1150-1156. doi:10.1038/nsmb1316

Rodriguez, J., Vernus, B., Chelh, I., Cassar-Malek, I., Gabillard, J. C., Hadj Sassi, A., Seiliez, I., Picard, B. and Bonnieu, A. (2014). Myostatin and the skeletal muscle atrophy and hypertrophy signaling pathways. *Cell. Mol. Life Sci.* **71**, 4361-4371. doi:10.1007/s00018-014-1689-x

Sabari, B. R., Dall'Agnese, A., Boija, A., Klein, I. A., Coffey, E. L., Shrinivas, K., Abraham, B. J., Hannett, N. M., Zamudio, A. V., Manteiga, J. C. et al. (2018). Coactivator condensation at super-enhancers links phase separation and gene control. *Science* **361**, eaar3958. doi:10.1126/science.aar3958

Shin, Y. and Brangwynne, C. P. (2017). Liquid phase condensation in cell physiology and disease. *Science* **357**, eaaf4382. doi:10.1126/science.aaf4382

Strom, A. R., Emelyanov, A. V., Mir, M., Fyodorov, D. V., Darzacq, X. and Karpen, G. H. (2017). Phase separation drives heterochromatin domain formation. *Nature* **547**, 241-245. doi:10.1038/nature22989

Sudol, M. (1994). Yes-associated protein (YAP65) is a proline-rich phosphoprotein that binds to the SH3 domain of the Yes proto-oncogene product. *Oncogene* **9**, 2145-2152.

Sudol, M., Bork, P., Einbond, A., Kastury, K., Druck, T., Negrini, M., Huebner, K. and Lehman, D. (1995). Characterization of the mammalian YAP (Yes-associated protein) gene and its role in defining a novel protein module, the WW domain. *J. Biol. Chem.* **270**, 14733-14741. doi:10.1074/jbc.270.24.14733

Sun, C., De Mello, V., Mohamed, A., Ortuste Quiroga, H. P., Garcia-Munoz, A., Al Bloshi, A., Tremblay, A. M., von Kriegsheim, A., Collie-Duguid, E., Vargesson, N. et al. (2017). Common and distinctive functions of the hippo effectors Taz and Yap in skeletal muscle stem cell function. *Stem Cells* **35**, 1958-1972. doi:10.1002/stem.2652

Suzuki, A., Scruggs, A. and Iwata, J. (2015). The temporal specific role of WNT/beta-catenin signaling during myogenesis. *J. Nat. Sci.* **1**, e143.

Tapon, N., Harvey, K. F., Bell, D. W., Wahrer, D. C., Schiripo, T. A., Haber, D. and Hariharan, I. K. (2002). salvador Promotes both cell cycle exit and apoptosis in Drosophila and is mutated in human cancer cell lines. *Cell* **110**, 467-478. doi:10.1016/S0092-8674(02)00824-3

Totaro, A., Castellan, M., Di Biagio, D. and Piccolo, S. (2018). Crosstalk between YAP/TAZ and Notch Signaling. *Trends Cell Biol.* **28**, 560-573. doi:10.1016/j.tcb.2018.03.001

Tripathi, S., Miyake, T. and McDermott, J. C. (2019). Smad7:beta-catenin complex regulates myogenic gene transcription. *Cell Death Dis* **10**, 387. doi:10.1038/s41419-019-1615-0

Udan, R. S., Kango-Singh, M., Nolo, R., Tao, C. and Halder, G. (2003). Hippo promotes proliferation arrest and apoptosis in the Salvador/Warts pathway. *Nat. Cell Biol.* **5**, 914-920. doi:10.1038/ncb1050

Varelas, X. (2014). The Hippo pathway effectors TAZ and YAP in development, homeostasis and disease. *Development* **141**, 1614-1626. doi:10.1242/dev.102376

Wackerhage, H., Del Re, D. P., Judson, R. N., Sudol, M. and Sadoshima, J. (2014). The Hippo signal transduction network in skeletal and cardiac muscle. *Sci. Signal.* **7**, re4. doi:10.1126/scisignal.2005096

Wada, K., Itoga, K., Okano, T., Yonemura, S. and Sasaki, H. (2011). Hippo pathway regulation by cell morphology and stress fibers. *Development* **138**, 3907-3914. doi:10.1242/dev.070987

Watt, K. I., Goodman, C. A., Hornberger, T. A. and Gregorevic, P. (2018). The hippo signaling pathway in the regulation of skeletal muscle mass and Function. *Exerc. Sport Sci. Rev.* **46**, 92-96. doi:10.1249/JES.0000000000000142

Wu, S., Huang, J., Dong, J. and Pan, D. (2003). hippo encodes a Ste-20 family protein kinase that restricts cell proliferation and promotes apoptosis in conjunction with salvador and warts. *Cell* **114**, 445-456. doi:10.1016/S0092-8674(03)00549-X

Yu, F. X., Zhao, B. and Guan, K. L. (2015). Hippo pathway in organ size control, tissue homeostasis, and cancer. *Cell* **163**, 811-828. doi:10.1016/j.cell.2015.10.044

Yu, M., Peng, Z., Qin, M., Liu, Y., Wang, J., Zhang, C., Lin, J., Dong, T., Wang, L., Li, S. et al. (2021). Interferon-gamma induces tumor resistance to anti-PD-1 immunotherapy by promoting YAP phase separation. *Mol. Cell* **81**, 1216-1230.e9. doi:10.1016/j.molcel.2021.01.010

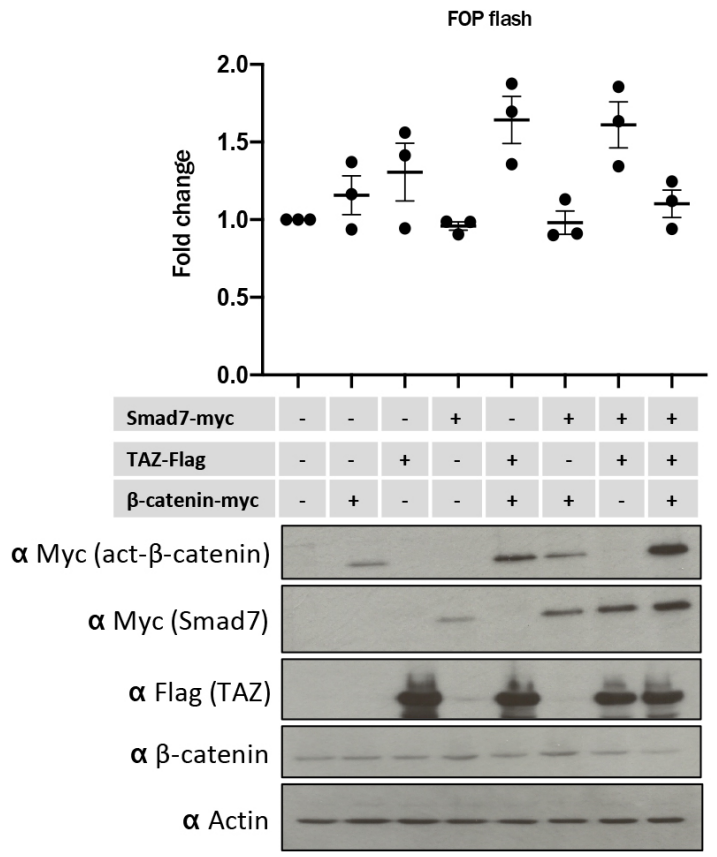

Fig. S1. Smad7-myc, TAZ-flag, β-catenin alone or in combination were ectopically expressed along with the FOP flash firefly luciferase reporter gene. *Renilla* luciferase served as the transfection control. Cells were harvested for dual Luciferase determination at 16 h post transfection. Normalized luciferase activity was compared to the control to determine fold changes. Lower panels indicate western blot analysis of the protein levels derived from the transfected plasmids. Each condition was compared to the control for the three individually transfected samples to determine fold changes. Each bar represents the mean of three technical replicates. The error bars represent standard error of the mean (SEM).

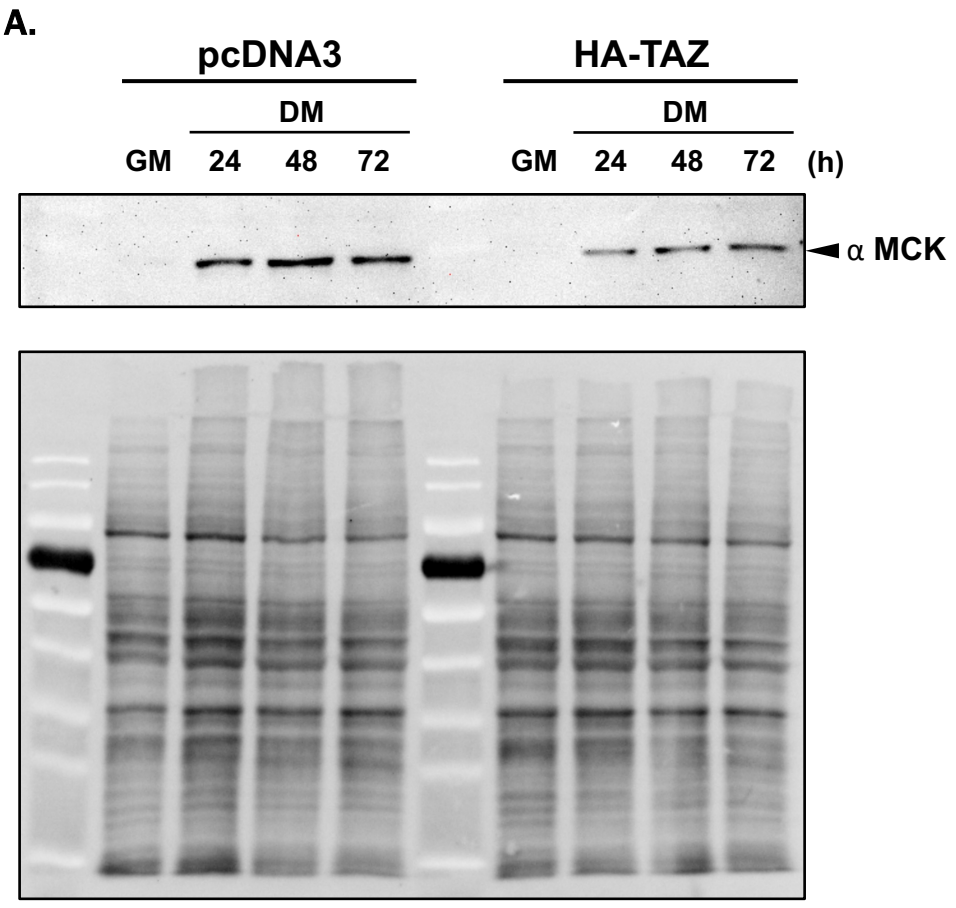

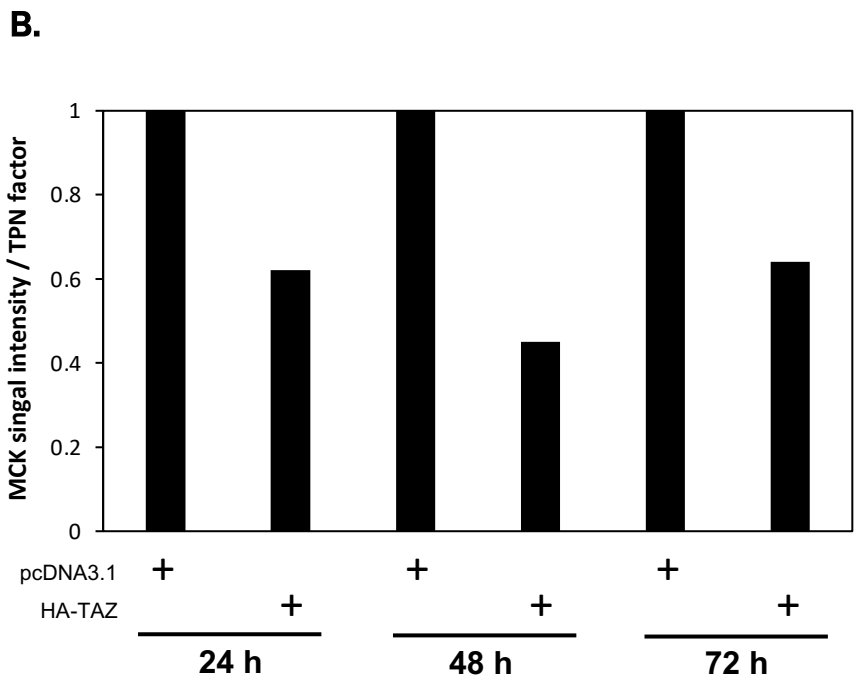

Fig. S2. HA-TAZ and pcDNA3 control were ectopically expressed in C2C12 and grown for 24 hours before switching to differentiation media for 24 to 72 h. Lysates were collected and assessed for expression of MCK by western blot analysis. MCK protein levels were quantified at each timepoint and normalized to the signal band intensity respective to total protein normalization (TPN) factor indicated in the gel image below the western blot. On the right side, a bar graph representing the TPN normalized MCK data at each timepoint is shown, indicating a downregulation of MCK protein levels in differentiating C2C12 cells transfected with TAZ compared to the corresponding control.

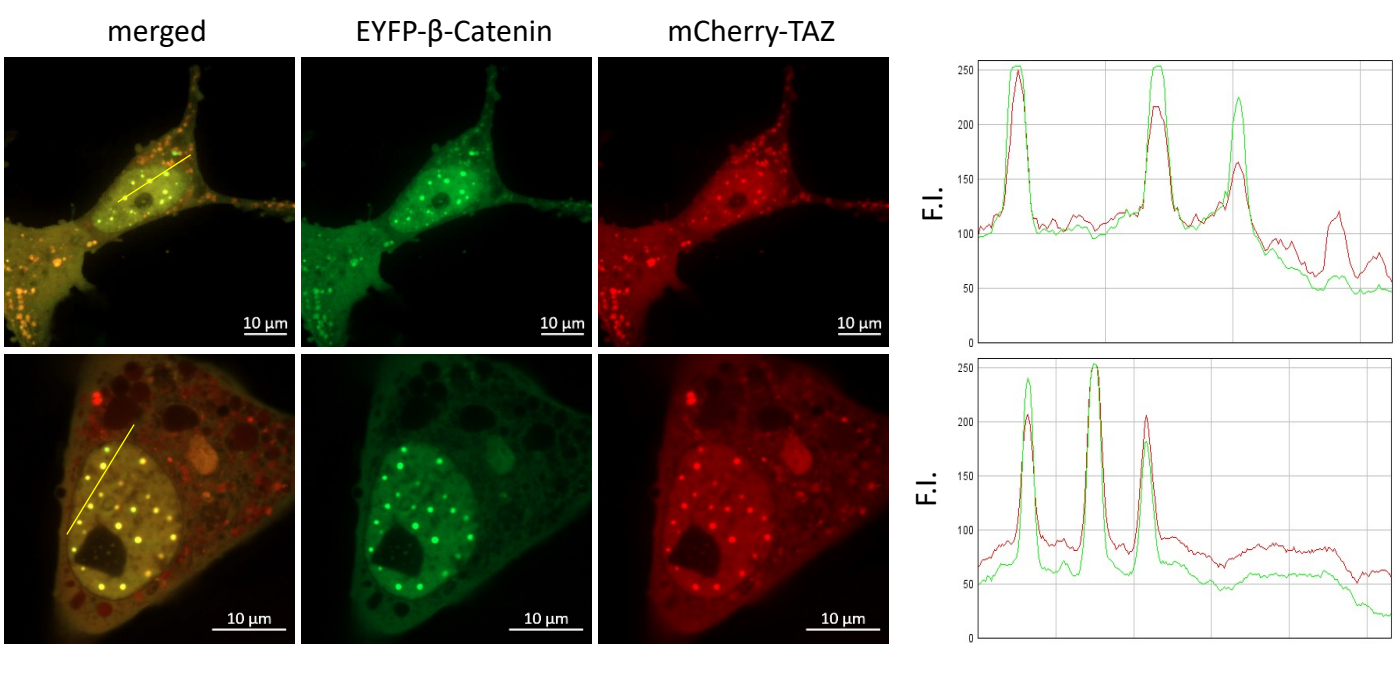

Fig. S3. C2C12 cells were transfected with indicated expression constructs. After 1 day, the cells were subjected to live-cell confocal fluorescence microscopy. The micrographs of samples were analyzed for co-localization by line-scan analysis for fluorescence intensity (F.I.) of green (EYFP-β-catenin) and red (mCherry-TAZ) using ImageJ.

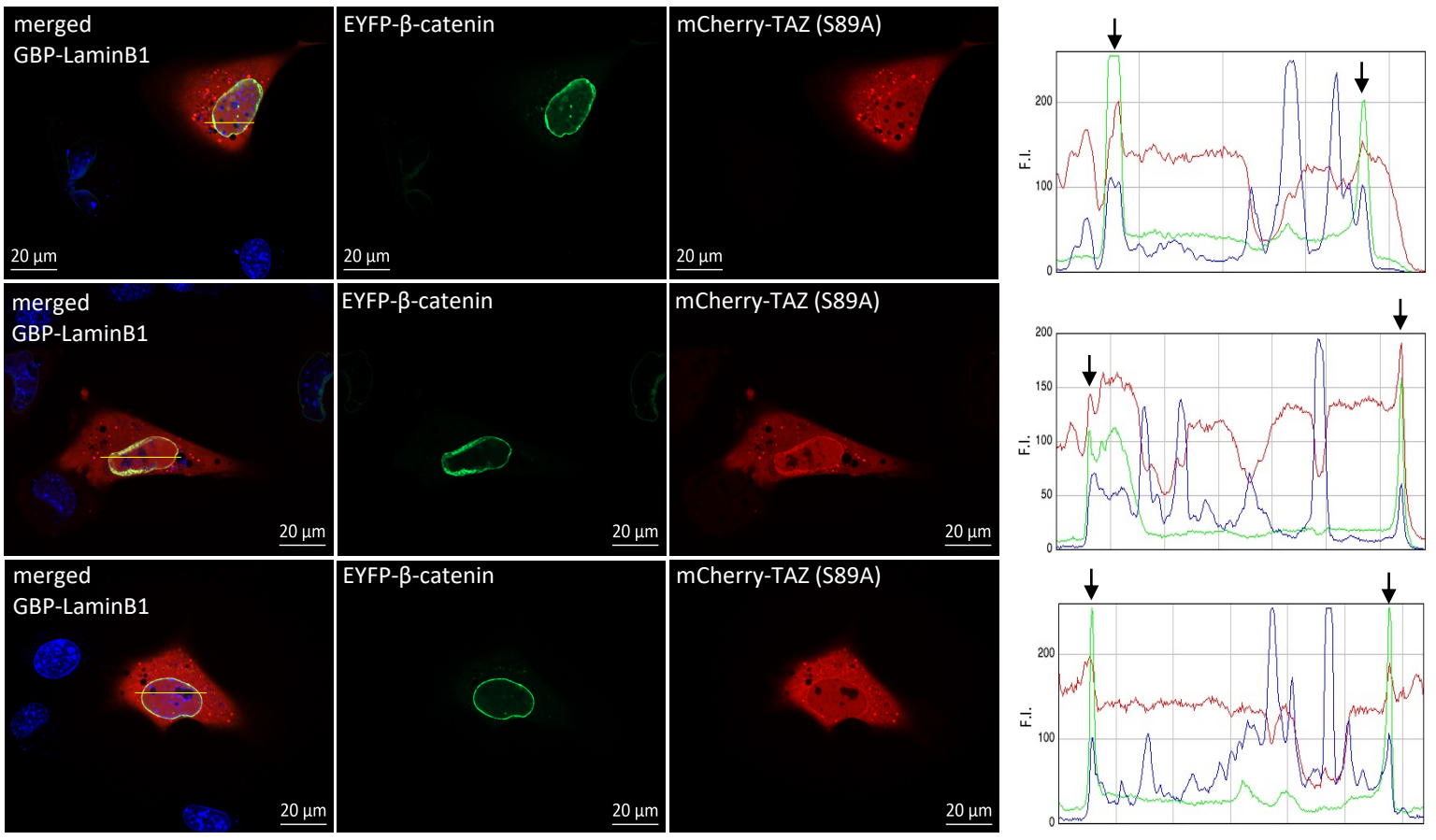

Fig. S4. C2C12 myogenic cells were transfected with the indicated expression constructs. After 1 day, the cells were subjected to live-cell confocal fluorescence microscopy. EYFP-β-catenin was localized to the nuclear envelop by an interaction trap using GBP-LaminB1. A line scan analysis along the indicated yellow line in the merged micrograph depicts recruitment of mCherry-TAZ to the nuclear envelope trapped EYFP-β-catenin, as indicated by arrows.

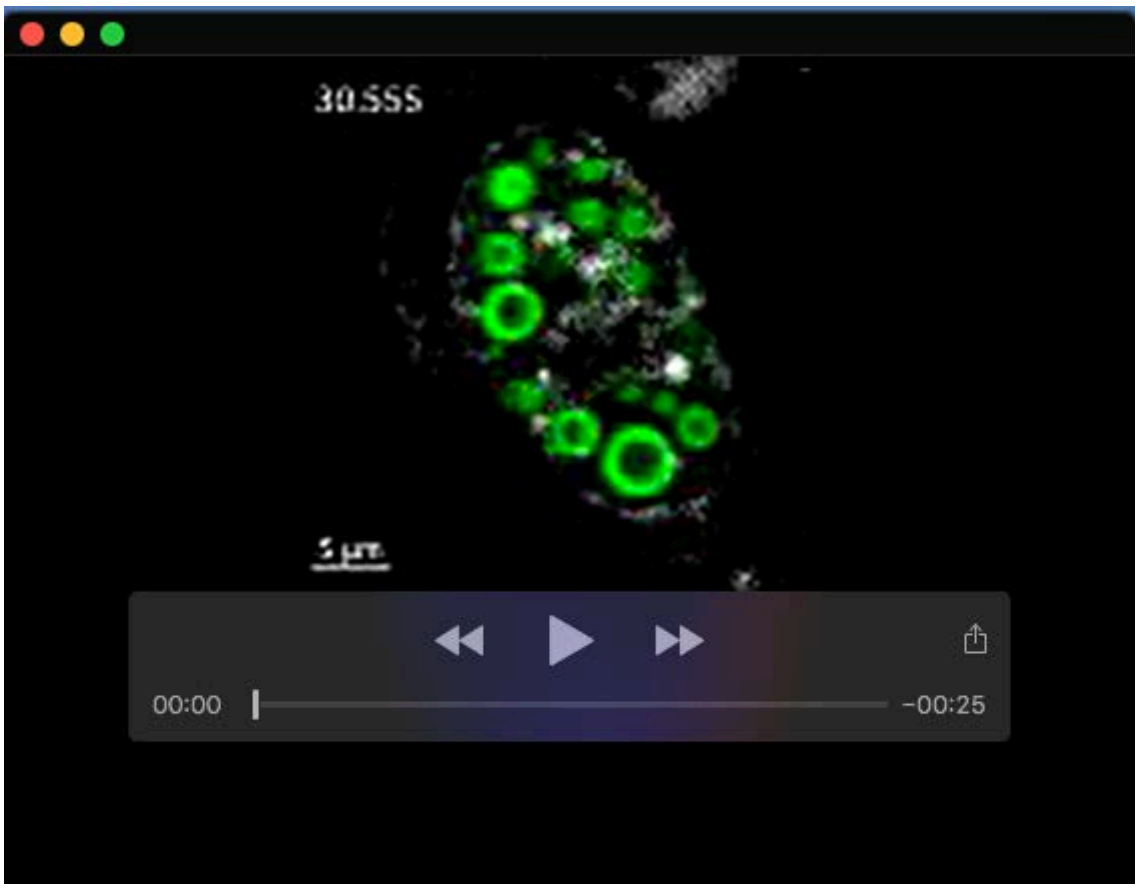

Movie 1. Time-lapse demonstration of nuclear condensate formation and fusion of EYFP-TAZ by live-cell imaging. Live cell spinning disk confocal imaging of ectopically expressed EYFP-TAZ (green) was carried out indicating the formation of spherical condensate structures inside the nucleus (imaged using Hoechst 33342 in blue). Videos document fusion properties of EYFP-TAZ condensates.

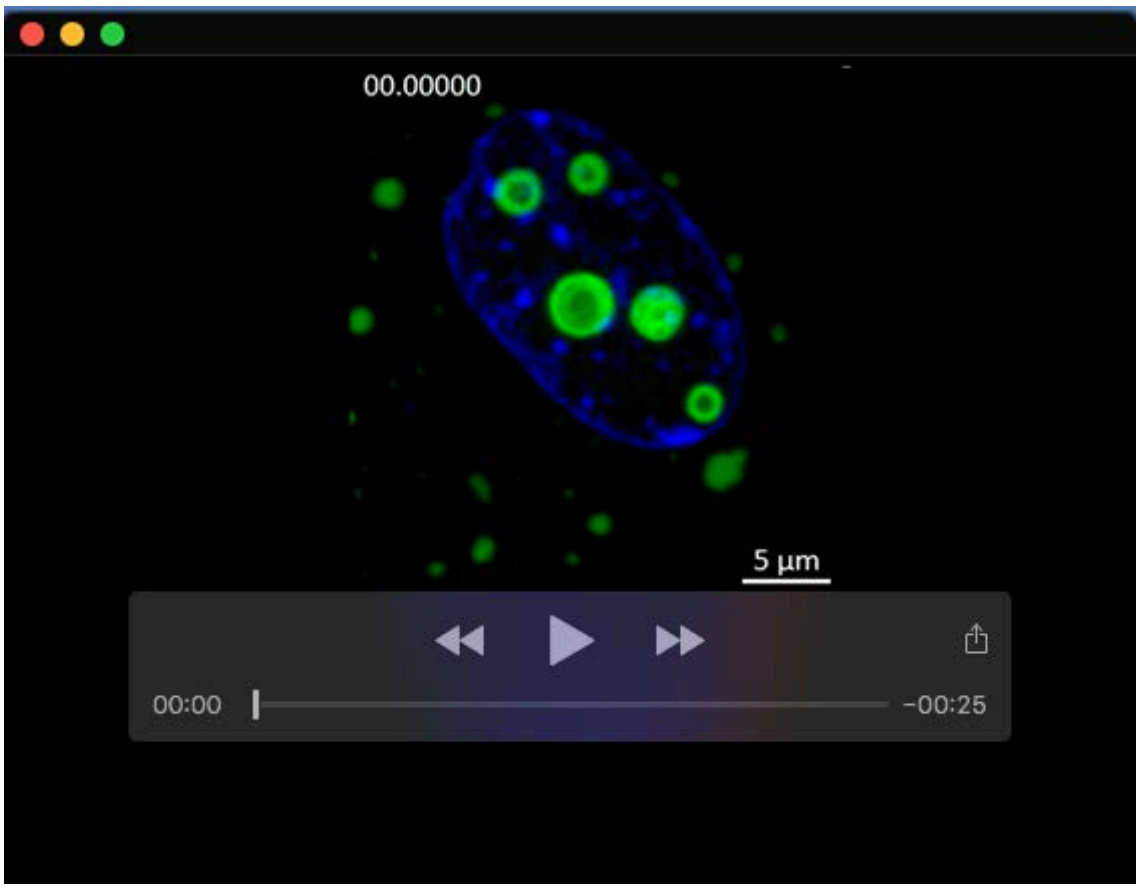

Movie 2. Time-lapse demonstration of nuclear condensate formation and fusion of EYFP-TAZ by live-cell imaging. Live cell spinning disk confocal imaging of ectopically expressed EYFP-TAZ (green) was carried out indicating the formation of spherical condensate structures inside the nucleus (imaged using Hoechst 33342 in white). Videos document fusion properties of EYFP-TAZ condensates.

Journal of Cell Science • Supplementary information